Published in final edited form as:
J Biol Chem. 2001 June 15; 276(24): 21303–21310.

Identification of Common Binding Sites for Calmodulin and Inositol 1,4,5-Trisphosphate Receptors on the Carboxyl Termini of Trp Channels*

Jisen Tang‡, **Yakang Lin**‡, **Zongming Zhang**‡, **Svetlana Tikunova**§, **Lutz Birnbaumer**¶, and **Michael Xi Zhu**‡,||

‡ *Neurobiotechnology Center, Ohio State University, Columbus, Ohio 43210*

§ *Department of Neuroscience and Department of Molecular and Cellular Biochemistry, Ohio State University, Columbus, Ohio 43210*

¶ *Departments of Anesthesiology, Biological Chemistry, and Molecular, Cellular, and Developmental Biology, UCLA, Los Angeles, California 90095*

Abstract

Homologues of *Drosophila* Trp (transient receptor potential) form plasma membrane channels that mediate Ca^{2+} entry following the activation of phospholipase C by cell surface receptors. Among the seven Trp homologous found in mammals, Trp3 has been shown to interact with and respond to IP_3 receptors (IP_3Rs) for activation. Here we show that Trp4 and other Trp proteins also interact with IP_3Rs. The IP_3R-binding domain also interacts with calmodulin (CaM) in a Ca^{2+}-dependent manner with affinities ranging from 10 nM for Trp2 to 290 nM for Trp6. In addition, other binding sites for CaM and IP_3Rs are present in the α but not the β isoform of Trp4. In the presence of Ca^{2+}, the Trp-IP_3R interaction is inhibited by CaM. However, a synthetic peptide representing a Trp-binding domain of IP_3Rs inhibited the binding of CaM to Trp3, −6, and −7 more effectively than that to Trp1, −2, −4, and −5. In inside-out membrane patches, Trp4 is activated strongly by calmidazolium, an antagonist of CaM, and a high (50 μM) but not a low (5 μM) concentration of the Trp-binding peptide of the IP_3R. Our data support the view that both CaM and IP_3Rs play important roles in controlling the gating of Trp-based channels. However, the sensitivity and responses to CaM and IP_3Rs differ for each Trp.

Binding of many cell surface receptors by hormones, neuro-transmitters, and growth factors leads to the activation of phospholipase C, which in turn produces diacylglycerol and inositol 1,4,5-trisphosphate (IP_3).1 Diacylglycerol activates protein kinase C, while IP_3 triggers Ca^{2+} release from internal Ca^{2+} stores by activating a set of intracellular Ca^{2+} release channels, referred to as IP_3 receptors (IP_3Rs). The release of Ca^{2+} from internal stores in turn activates store-operated channels (SOCs) located on the plasma membrane, allowing Ca^{2+} influx from the extracellular space. The store-operated Ca^{2+} influx, also known as capacitative Ca^{2+} entry (1,2), plays critical roles in controlling the duration and the frequency of cytosolic Ca^{2+} changes (2–4).

In contrast to the well defined roles of IP_3 and IP_3Rs in Ca^{2+} release, the molecular makeup of channels that mediate Ca^{2+} influx and their gating mechanism(s) remain to be elucidated. *Drosophila* transient receptor potential (Trp) protein and its mammalian homologues have been

*The work was supported in part by National Institutes of Health Grants GM54235 (to M. X. Z.) and HL45198 (to L. B.).

|| To whom all correspondence should be addressed: The Ohio State University Neurobiotechnology Center, 168 Rightmire Hall, 1060 Carmack Rd., Columbus, OH 43210. Tel.: 614-292-8173; Fax: 614-292-5379; E-mail: zhu.55@osu.edu..

shown to form either Ca^{2+} selective or nonselective cation channels that mediate Ca^{2+} influx in response to phospholipase C activation (5–7). To date, seven *trp* genes have been cloned from mammalian species (6,8), probably reflecting the heterogeneity of Ca^{2+} influx channels or pathways found in different cells (4,9). Expression of individual Trp proteins in heterologous systems revealed that Trp channels may be activated by a number of intermediaries involved in the phospholipase C-stimulated signaling cascade, including Ca^{2+} (10), diacylglycerol (11), and activated IP_3Rs (12–14). Although store depletion induced by an intracellular Ca^{2+}-ATPase inhibitor, thapsigargin, appears to be sufficient to open some Trp channels (*e.g.* Trp1 (15), Trp2 (16), and Trp4 (17)), it remains controversial whether all Trp proteins participate in forming SOCs (18,19). Perhaps the answer lies within the structural organization of the channel, which could be composed of four different Trp subunits (5). A recent example showed that coexpression of two *Drosophila* store-insensitive Trp proteins, Trp*γ* and Trp-like (TrpL), led to the formation of a SOC (20). Thus, the store sensitivity may be reconstituted with the proper combination of different Trp subunits. Consistent with this idea, Trp1, Trp3, and Trp4 have been shown to be part of SOCs in human submandibular gland cells, neurons, and adrenal cortex cells, respectively (15,21,22).

Recent studies showed that IP_3Rs are involved in the activation of Trp3. Following the initial demonstration that human Trp3 (hTrp3) in inside-out membrane patches was activated by IP_3Rs in the presence of IP_3 (12), Boulay *et al.* (14) identified the binding domains involved in the Trp-IP_3R interaction, which were found to be located in the N terminus of type 3 IP_3R (IP_3R3) and the C terminus of Trp3. Overexpression of short peptide fragments containing these binding sites altered the activity of endogenous store-operated Ca^{2+} influx in HEK293 cells (14). While the association with IP_3Rs has also been shown for Trp1 and Trp6 by coimmunoprecipitation (14,23,24), it remains to be determined whether direct interaction with IP_3Rs is common for all Trp proteins. In this study, we examined murine Trp4 (mTrp4) for interaction with the first and the stronger Trp3-binding domain of IP_3R3 (F2q; Glu^{669}–Asp^{698}) (14). In addition, we examined the interaction between Trp4 and calmodulin (CaM), which has been shown to bind to the C termini of *Drosophila* Trp (25) and TrpL (26,27) and has been implicated to cause inactivation of TrpL (28). We report here the presence of two CaM-binding and at least two IP_3R3-binding sites at the C terminus of Trp4. The first CaM-binding site overlaps closely with one of the IP_3R3-binding site. Common binding sites for CaM and IP_3Rs also exist in other Trp proteins. In functional studies, we show that currents are activated in inside-out membrane patches excised from Trp4-expressing HEK293 cells by calmidazolium (CMZ), an antagonist of CaM, and by a peptide representing one of the Trp-binding domains of IP_3R3.

MATERIALS AND METHODS

DNA Constructs

Fragments of IP_3Rs and Trps were generated by polymerase chain reaction (PCR). All sense primers contain an *Nco*I recognition site at the 5′ with ATG in frame with the codon for the first amino acid. The antisense primers start with an A nucleotide followed by the antisense codon for the last amino acid. PCR products were subcloned into pCRII (Invitrogen), and nucleotide compositions were confirmed by DNA sequencing. Glutathione *S*-transferase (GST) fusion constructs were made by subcloning *Nco*I/*Eco*RI fragments into a modified pGEX4T-1 vector (Amersham Pharmacia Biotech), in which an *Nco*I site was added after the *Bam*HI site. By design, the insert in each fusion protein starts with a Met and ends with a “TAA” stop codon (T comes from the A in the antisense primer, while AA comes from the pCRII vector). Complementary DNA for enhanced blue fluorescence protein (EBFP) was excised from pEBFP-C1 (CLONTECH) and sub-cloned into pAGA (29) at *Nco*I/*Sma*I sites, while that for maltose-binding protein (MBP) was amplified from pMAL-C2 (New England

Biolabs) by PCR, excised with *Mfe*I/*Nco*I, and subcloned into pAGA at *Eco*RI/*Nco*I sites. Constructs for EBFP fusion proteins contained inserts downstream from the EBFP coding region and were made using existing restriction sites on mouse *trp*4 at the 5′-end and *Xba*I at the 3′-end. MBP fusion proteins contain the first 322 residues of MBP followed by inserts, of which the cDNAs were subcloned into *Nco*I/*Eco*RI sites.

In Vitro Binding Experiments

Preparation of GST fusion proteins; ^{35}S-labeled CaM, EBFP, and MBP fusion proteins; and procedures for pull-down experiments are as described (30). For interaction with CaM, CaM-Sepharose (Amersham Pharmacia Biotech) was used. The binding buffer used for IP_3R3-Trp interaction contains 100 mM KCl, 2 mM $MgCl_2$, 0.5% Lubrol, and 20 mM Tris-HCl, pH 7.5. The buffer used for CaM-Trp interaction generally contains 120 mM KCl, 0.5% Lubrol, 20 mM Tris-HCl, 10 mM EGTA, 9.96 mM $CaCl_2$. pH was adjusted to 7.5. The estimated free Ca^{2+} concentration for the buffer is 10 μM. However, because EGTA is a poor buffer for Ca^{2+} concentration at the micromolar range, the actual free Ca^{2+} concentration of this buffer is about 70 μM as determined by spectrofluorometric measurements using Fura2FF (TEF Laboratories, Austin, TX) as a low affinity Ca^{2+} indicator and HEDTA-buffered solutions as standards.

For the determination of Ca^{2+}-dependence of Trp binding to CaM, HEDTA or nitrilotriacetic acid instead of EGTA was used, and total $CaCl_2$ was added according to the MaxChelator program (C. Patton, Stanford University) to give rise to desired free Ca^{2+} concentrations. ^{35}S-Labeled MBP fusion proteins containing the CaM-binding sites were incubated with CaM-Sepharose at room temperature for 30 min in varying free Ca^{2+} concentrations. Each sample was washed twice with the same binding buffer that was used for the incubation; thus, the free Ca^{2+} concentration was kept unchanged. Bound proteins were subjected to SDS-polyacrylamide gel electrophoresis. The radioactivity of [^{35}S]MBP fusion proteins retained was quantified by phosphorimaging analysis. The percentage of maximal increase over the value obtained in 10 mM EGTA with no added Ca^{2+} was fitted with the Hill equation $I/I_{max} = C^n/(C^n + (K_{½})^n)$, where I/I_{max} represents the relative binding, C is the Ca^{2+} concentration, n is the Hill coefficient, and $K_{½}$ is the Ca^{2+} concentration that gives rise to half-maximal binding.

For competition studies, recombinant human CaM was prepared from bacterial lysate using phenyl-Sepharose (Sigma) as described (31). Peptide F2v (EYLSIEYSEEEVWLTWTD) was synthesized by Research Genetics. CaM or peptide F2v, in the desired final concentrations, was included in the binding and washing buffers containing 50 or 70 μM free Ca^{2+}.

Affinity Measurement for Trp-CaM Interaction

All fluorescence measurements were performed on a PerkinElmer Life Sciences LS5 Spectrofluorometer at 22 °C. Peptides for CaM-binding sites of Trp1–7 were synthesized by Waterloo Peptide Synthesis (University of Waterloo, Ontario, Canada). Peptide for the second CaM-binding site of mTrp4α was synthesized by the Tufts University Core Facility (Tuft University, Boston, MA). Phosphodiesterase activity was assayed by monitoring the hydrolysis of fluorescent 2′-methylanthraniloyl cGMP (8 μM) in 1 ml of solution containing 200 mM MOPS, pH 7.0, 90 mM KCl, 3 mM $MgCl_2$, 2 mM EGTA, 100 μM free Ca^{2+}, 25 nM CaM, and the desired amount of peptide. Samples were excited at 330 nm, and emission at 450 nm was measured. The dissociation constant (K_d) with Ca^{2+}/CaM was calculated from the activation curves of phosphodiesterase by CaM in the absence and the presence of the peptide as described (32).

Cell Lines and Electrophysiology

HEK293 cells stably expressing mTrp4 (T4-1 and T4-60 cells) and culture conditions were as described (33). Cells were seeded in 35-mm dishes 2 days prior to patch clamp recordings. Conditions for recording from inside-out patches were essentially as described (34). The pipette solution contained 140 mM Na-Hepes, 5 mM NaCl, and 2 mM $CaCl_2$, pH 7.5. Inside-out patches were excised from the Trp4 cells into a Ca^{2+}-free intracellular solution containing 140 mM potassium gluconate, 5 mM NaCl, 1 mM $MgCl_2$, 5 mM EGTA, 10 mM Hepes, pH 7.5. CMZ, CaM, and peptide F2v were diluted to the final concentration in the intracellular solution containing no Ca^{2+} (for F2v) or 18 μM free Ca^{2+} (for CMZ) and were applied to the cytoplasmic side of excised patches through perfusion. A step protocol containing continuous alternating steps to 40 and −40 mV, each for 1 s, from holding at 0 mV was applied throughout the experiments. Currents were recorded at sampling frequency of 5 kHz and filtered at 1 kHz. Currents recorded at −40 mV from 100 episodes under each condition were averaged using pCLAMP 8 (Axon Instruments) after digital filtering at 500 Hz and base-line adjustment.

RESULTS

The C Terminus of Trp4 Binds to IP_3R3 and CaM

A previous study showed that a GST fusion protein containing the F2q fragment of human IP_3R3 (Glu^{669}–Asp^{698}) interacted with the C terminus of hTrp3 (14). The Trp3 peptides shown to interact with IP_3R3 were T3C7 (Met^{742}–Glu^{795}) and T3C8 (Gln^{777}–Asp^{797}). T3C8 bound to IP_3R3 more weakly than T3C7 and thus represents a partial IP_3R-binding domain of Trp3. Because the sequence homology at the regions that align to T3C7 is relatively low (13, 13, and 17% identical between Trp3 and Trp1, Trp2, and Trp4, respectively), it was difficult to predict whether the IP_3R-binding domain is conserved among all Trp homologues. Therefore, we tested the binding of GST-IP_3R3F2q to mTrp4. ^{35}S-Labeled MBP and EBFP fusion proteins containing the N and C terminus of mTrp4, respectively, were synthesized *in vitro* and incubated with GST or GST-IP_3R3F2q bound to glutathione-Sepharose. Fig. 1*A* shows the Trp4 regions present in the fusion proteins, and Fig. 1*B* shows that while MBP (*M*) or EBFP (*E*) alone and MBP-Trp4 N terminus (*NT*) have no specific interaction with IP_3R3F2q, the EBFP-Trp4 C-terminal fusion protein (*CT*) binds to GST-IP_3R3F2q. To examine the interaction between Trp4 and CaM, we incubated the fusion proteins with CaM-Sepharose. Only EBFP-T4CT (*CT*) interacted with CaM. The binding of T4CT to CaM was very weak in the absence of Ca^{2+}, but in the presence of 70 μM Ca^{2+}, it was greatly increased (Fig. 1*B*).

We divided T4CT into two portions. CT1 (residues 659–750) includes the sequence homologous to T3C7 of Trp3, while CT2 (residues 733–974) contains the more C-terminal sequence unique to Trp4. Interestingly, both CT1 and CT2 bind strongly to GST-IP_3R3F2q and to Ca^{2+}/CaM. Another N-terminal construct (*NT1*) and the transmembrane region (*TM*) of Trp4 did not interact with IP_3R3F2q or Ca^{2+}/CaM (Fig. 1*C*). The over-lapping sequence between CT1 and CT2 is relatively conserved among the Trp homologues (11 out 20 amino acids are identical between Trp3 and Trp4). However, an EBFP fusion protein containing this sequence (C*f*) did not interact with either IP_3R3F2q or Ca^{2+}/CaM (Fig. 1*D*). On the other hand, a construct that contains mostly the sequence equivalent to T3C7 but not T4C*f* (C*c*) interacted with both IP_3R3F2q and Ca^{2+}/CaM. These results indicate that just as T3C7, a similar region at the C terminus of Trp4 also binds to IP_3R3. In addition, there is at least one additional IP_3R-binding site more C-terminal to the previously defined site. Moreover, both IP_3R-binding regions bind to Ca^{2+}/CaM.

The First CaM-binding Site of Trp4 Closely Overlaps with an IP_3R-binding Site

To determine how close the first CaM-binding site of Trp4 is to the site that binds to IP_3R3F2q, we produced MBP- and EBFP-fusion proteins containing smaller fragments of T4C*c* and tested

their binding to GST-IP_3R3F2q and Ca^{2+}/CaM. Fig. 2 shows the composition of the fusion proteins and the binding results. In general, Trp4 fragments that bound to IP_3R3F2q also bound to Ca^{2+}/CaM. The smallest fragment that binds to IP_3R3F2q and Ca^{2+}/CaM with nearly the same strength as T4C*c* is T4C*w* (Arg^{695}–Glu^{724}). Removing two residues from either the N or the C terminus of T4C*w* reduced the interaction with both IP_3R3F2q and Ca^{2+}/CaM (Fig. 2*C*, T4C*v* and T4C*x*). Smaller fragments, such as C*a*, C*aa*, and C*ab*, had much weaker binding to IP_3R3F2q, and this was also accompanied by greatly reduced binding to Ca^{2+}/CaM. Therefore, the binding sites for CaM and for the IP_3R cannot be separated by deletion studies, indicating that a common sequence, referred to as the CaM/IP_3R binding (CIRB) domain, is involved in the interaction with CaM and with the IP_3R.

The Second CaM-binding Site Is Present in Trp4α but Not Trp4β

The minimal domains that bind to CaM and IP_3R3F2q at the CT2 region were sought in a similar manner (Fig. 3). However, it appears that the CT2 IP_3R-binding domain is not confined to a short sequence like the CIRB domain. When CT2 was divided into CT2a and CT2b, both retained weak interaction with IP_3R3F2q (Fig. 3*B*). Further analyses suggested that the region from Gly^{781} to Ser^{864} retains significant binding to IP_3R3F2q (Fig. 3*C*). Interestingly, molecular cloning and immunoblot analysis have revealed the presence of two major isoforms of Trp4, Trp4*α* and Trp4*β* (33). The *β* form lacks the 84 amino acids corresponding to Gly^{781}–Ser^{864} of the *α* form. Thus, CT2*β* binds very weakly to IP_3R3F2q (Fig. 3*B*).

In contrast to IP_3R3F2q, CaM binds to a short, confined sequence in CT2, CT2p (Arg^{787}–Asn^{812}, Fig. 3, *C* and *D*). Removing two residues from its N terminus (CT2r) nearly abolished the binding, whereas removing two residues from its C terminus (CT2q) reduced the binding by 45%, as determined by phosphorimaging analysis from two independent experiments. Although CT2p is contained within the CT2 IP_3R3F2q-binding region, it does not bind to the IP_3R fragment. Therefore, the binding sites for CaM and IP_3R3F2q in the CT2 region do not overlap as closely as the CIRB sequence. Because the CaM binding site is not present in TRP4*β*, CT2*β* does not bind to Ca^{2+}/CaM (Fig. 3*B*).

CIRB Domain Is Conserved among Trp Proteins

As shown in Fig. 4, regions equivalent to T4C*w* from hTrp1, mTrp2, hTrp3, mTrp5, mTrp6, mTrp7, and *Drosophila* Trp and TrpL also interacted with both GST-IP_3R3F2q and Ca^{2+}/CaM. For TrpL, the CIRB domain is in addition to the two CaM-binding sites (710–725, 854–875) identified previously (26,27). For *Drosophila* Trp, the CIRB domain is within a previously reported CaM-binding region (683–976) (25). For Trp3, the CIRB domain is the only CaM-binding domain, because deletion of this site eliminated the binding and the regulation of Trp3 activity by Ca^{2+}/CaM (34). This may also be the case for Trp6 and Trp7, since they are very similar to Trp3. Trp1 terminates soon after the CIRB sequence and therefore is unlikely to have a second binding site at the C terminus. The C-terminal sequence of mTrp2 (residues 944–1072) and of mTrp5 (residues 762–975) interacted with both Ca^{2+}/CaM and GST-IP_3R3F2q (not shown), suggesting that the second binding sites for the two modulators are conserved in Trp2, Trp4*α*, and Trp5, despite the fact that the homology among the three Trps is very low at these regions.

Using synthetic peptides representing the CIRB domains of Trp1–7 and the second CaM-binding site of Trp4, we determined the affinities to range from 10 nM for mTrp2 to 290 nM for mTrp6 (Table I). The second CaM-binding site of Trp4 has lower affinity (600 nM) than the CIRB domains of all Trp proteins. The apparent affinities for Ca^{2+}, as measured by *in vitro* binding assays using [^{35}S]MBP-Trp fusion proteins and CaM-Sepharose, differed greatly from 1.0 μM for the second CaM-binding site of Trp4 to 44.2 μM for the CIRB domain of Trp5

(Table I). The Hill coefficients of Ca^{2+} dependence for the CaM-Trp interactions were about 1.5–3.5.

All IP_3Rs Interact with Trp3

Just as the CIRB domain is conserved in all Trp homologues, the F2q Trp-binding site is also conserved in the three known mammalian IP_3Rs. Fig. 5*A* shows that regions homologous to IP_3R3F2q from IP_3R1 and IP_3R2 also interacted with the C terminus of Trp3. The alignment of the three sequences indicates that only the C-terminal halves are conserved. Further experimentation using smaller segments of IP_3R3F2q fused to GST showed that the C-terminal half of F2q (represented by F2v) is the minimal domain of IP_3R3 that interacts with Trp3 (Fig. 5*B*).

Competition between CaM and IP_3R3 for Binding to Trps

In *in vitro* binding assays, we have shown that for T3C7, the interaction with IP_3R3F2q was inhibited by purified recombinant human CaM and the binding to CaM was blocked by a synthetic peptide, composed of the sequence of F2v (34). Peptide F2v appears to be a potent inhibitor for CaM binding to Trp3, because the competition was observed in a binding buffer that contained Ca^{2+}, a condition under which CaM has a high affinity for Trp3. In order to learn the relative abilities of CaM to compete with the IP_3R for binding to different Trps, we tested the competition between CaM and IP_3R3F2q for binding to the CIRB domains of other mammalian Trp homologues. The addition of CaM reduced the binding of ^{35}S-labeled MBP-T4C*w* to GST-IP_3R3F2q in a dose-dependent manner, with 50% inhibition (IC_{50}) occurring at 2.1 μM (Fig. 6*A*), similar to the value obtained for Trp3 (1.2 μM) (34). The inhibition of the Trp4-IP_3R3 interaction by 20 μM CaM was about 73%, slightly less than that of Trp3-IP_3R3 interaction (88%) (34). In addition, 20 μM CaM also inhibited the interaction between IP_3R3F2q and the CIRB domains of Trp1, −2, −5, −6, and −7 to various degrees (Fig. 6*B*). The effect of CaM was Ca^{2+}-dependent, since the inhibition by CaM was not observed in a Ca^{2+}-free binding buffer (Fig. 6*B*). These results indicate that at high Ca^{2+} concentrations, CaM competes with IP_3Rs for binding to the CIRB domains of all Trp proteins. However, the extent of inhibition varies from Trp to Trp, which is probably related to the differences in their affinities to CaM. Although the CT2 IP_3R-binding site does not overlap as closely to the CaM-binding site as the CIRB sequence, the binding between CT2c and IP_3R3F2q was also blocked by CaM (Fig. 6*C*).

Peptide F2v blocked the interaction between CaM and the CIRB domain of Trp1–7 with IC_{50} values ranging from 1.7 to 90 μM (Fig. 6*D*). The peptide is more effective in inhibiting the interaction between CaM and Trp3, −6, and −7 than that between CaM and Trp1, −2, −4, and −5. The effect of the peptide is specific because the binding of CaM to Trp4CT2k (residues 781–814), which does not interact with IP_3R3F2q (not shown), was not inhibited (Fig. 6*D*).

Peptide F2v and a CaM Antagonist Activate Trp4 in Excised Inside-out Patches

CaM bound to the CIRB domain has a general inhibitory function on Trp3, because in inside-out patches excised from HEK293 cells expressing Trp3, removing or inactivating CaM led to a large increase in Trp3 activity (34). In the absence of Ca^{2+} and at 5 μM, peptide F2v activated Trp3 by competing with CaM for binding to the CIRB domain. The activated channel was blocked by CaM (34). Consistent with the finding that F2v was 10 times less effective in competing with CaM for binding to Trp4 than to Trp3 (Fig. 6*D*), we found that in inside-out patches, F2v was also less potent in activating Trp4 than Trp3 (Fig. 7*A*). At 5 μM, F2v only caused a small increase in Trp4 activity, which is significantly different ($p < 0.05$) from the basal activity in one Trp4 cell line (T4-1) but not in the other one (T4-60). When the concentration of F2v was increased to 50 μM, both cell lines showed significant increase in activity ($p < 0.01$), which is more than 6 times higher than that stimulated by 5 μM F2v.

Additionally, patches excised from Trp4 cells were activated by 1 and 10 μM CMZ (Fig. 7*B*). Under the same conditions, untransfected HEK293 cells did not show any significant increase in activity after treatment with peptide F2v or CMZ (Fig. 7, *A* and *B*).

DISCUSSION

The mechanism of activation for SOCs remains mysterious. Three major hypotheses have been proposed. The first assumes that a small diffusible soluble factor capable of stimulating SOCs appears in the cytosol upon store depletion. Although it has been shown that acid extracts from activated Jurkat cells and platelets or a Ca^{2+} store-depleted mutant yeast strain contain such a factor, which when applied to naive cells could stimulate Ca^{2+} influx (35,36) or cation conductance (37), the identity of the Ca^{2+} influx factor has not been determined. The second hypothesis claims that a secretion-like process involving the insertion of channel-containing vesicles into the plasma membrane is required for activating SOCs (38). In agreement with this is the finding that actin redistribution affected capacitative Ca^{2+} entry (39). The third hypothesis is called conformational coupling and is modeled after the well known mechanism of excitation-contraction coupling between the L-type Ca^{2+} channel and the ryanodine receptor in skeletal muscle (40). In this case, IP_3Rs are thought to serve not only as channels for Ca^{2+} release but also as sensors for store depletion. The signal of store depletion is sent to the plasma membrane Ca^{2+} entry channels via a direct protein-protein interaction (2,41). Consistent with this hypothesis, it has been demonstrated that IP_3 activates cation channels on the plasma membranes of endothelial cells, macrophages and A431 epithelial cells (42–44) and that the activity of IP_3R1 purified from rat cerebellum is modulated by luminal Ca^{2+} (45).

Despite the controversy about whether or not Trp proteins form SOCs, accumulating evidence has indicated that IP_3 and IP_3Rs are involved in the activation of SOCs as well as Trp3 (12–14,46). Also, just like the native SOCs, Trp3 activation was prevented by actin filament condensation induced by ca-lyculin A, a phosphatase inhibitor (46). Therefore, the conformational coupling mechanism, and perhaps the secretion-like coupling mechanism as well, are applicable to Trp-based channels. Using molecular and biochemical approaches, Boulay *et al.* (14) identified the interacting domains of Trp3 and IP_3R3 and showed that they are involved in the regulation of native SOCs. In the current study, we further demonstrate that the interactions between Trp and IP_3R are common for all Trp proteins and for all IP_3Rs. Thus, conformational coupling involving direct physical interaction with activated IP_3Rs may be a common mechanism for the activation of Trp-based channels. Moreover, we show that the IP_3R-binding domains of the Trp proteins also bind to Ca^{2+}/CaM and that the binding by CaM inhibits the association between Trp and IP_3Rs. Therefore, the competition between CaM and IP_3Rs for binding to a common site may play a key role in controlling the gating of Trp-based channels. Based on the functional study of Trp3 using inside-out membrane patches and a non-Ca^{2+}-binding CaM mutant, we concluded that at rest, CaM is tethered to the channel and prevents it from being spontaneously active (34). Maneuvers that displaced CaM from Trp3 strongly activated the channel (34). Here, we show that Trp4 is also strongly activated by inactivating CaM with CMZ, indicating that CaM probably plays the same inhibitory role in all Trp-based channels. Consistent with this, CMZ also activates current in patches excised from cells expressing Trp1 or Trp6 (not shown). Thus, binding to CaM is essential to prevent the spontaneous activity of Trp channels.

Analysis of genomic sequences revealed that for hTrp1, hTrp4, hTrp5, *Drosophila* Trp, and TrpL, the coding sequence for the N-terminal end of the CIRB domain coincides with the beginning of an exon,[2] indicating that conformational coupling involving binding by IP_3Rs and its regulation by CaM were acquired early in evolution and that there may be a constraint

[2]M. X. Zhu, unpublished observation.

to preserve these modes of regulation for Trps. However, the IP_3R-deficient *Drosophila* photoreceptors showed normal response to light and unaltered function of Trp and TrpL (47, 48), suggesting that the *Drosophila* IP_3R is not involved in activating these channels. The fact that *Drosophila* Trp and TrpL interacted with human IP_3R3F2q fragment *in vitro* does not implicate a similar interaction *in vivo*. Interestingly, a comparison between the *Drosophila* IP_3R and the human IP_3R3 showed a very low homology between the two at the F2q region. An extra 38-amino acid sequence in the *Drosophila* IP_3R (725–762) essentially disrupts an otherwise intact F2q region. In addition, the *Drosophila* sequence contains only one of the two tryptophans critical for binding to Trp3 (34). Therefore, it is unlikely that the *Drosophila* IP_3R would be involved in activating the Trp channels in the same manner as its mammalian counterparts. Since only a single gene for IP_3R is present in the *Drosophila* genome (48), it is possible that in the insect's photoreceptors, a different protein would compete with CaM for binding to the CIRB domains of Trp and TrpL and hence activate the channels. Furthermore, the mechanism present here is only one of the several ways by which the Trp channels are activated. The involvement of IP_3Rs in the activation of mammalian Trps does not rule out the participation of other molecules in Trp gating.

In addition to the CIRB domain, binding sites for CaM and IP_3Rs are present downstream in Trp2, Trp4α, and Trp5, suggesting that subtype-specific functions carried by CaM and IP_3Rs also exist and contribute to the diversity in the regulation of Trp-based channels. Interestingly, the last 240 amino acids of human Trp4α including the 84-amino acid region that contains the binding sites for CaM and IP_3Rs are encoded by a single exon.[2] In Trp4β, the 84-amino acid region is deleted through the use of alternative splicing sites, and thus the second binding sites for CaM and IP_3Rs are not present. Surprisingly, the same region was recently shown to bind to the C terminus of IP_3Rs (49). It remains to be determined how the bindings of the N and C terminus of IP_3Rs and CaM to this region affect the function of Trp4α and how they differ from bindings to the more upstream CIRB domain.

Diversity also arises from the differences in the affinities of CIRB domains of different Trp homologues for CaM and for IP_3Rs. The affinities for CaM differ by as much as 29-fold between the CIRB domains of Trp2 and Trp6 (Table I). Because peptide F2v is more effective in displacing CaM from Trp3 and the closely related Trp6 and Trp7 than from the CIRB domain of other Trps, the affinities of the CIRB domains for the Trp-binding site of IP_3R3 may also be very different. In the context of conformational coupling, one important step accomplished by IP_3Rs is to displace the inhibitory CaM from the CIRB domain. This may be accomplished mainly by the binding of the F2v domain of IP_3R3 and homologous regions of IP_3R1 and IP_3R2. The effectiveness of the F2v may be dependent on local Ca^{2+} concentrations, since Trp binding to CaM is greatly enhanced by Ca^{2+}. In the binding assay shown in Fig. 6*D*, 70 μM free Ca^{2+} was used to facilitate the detection of CaM binding. Under this condition, peptide F2v blocked CaM binding to the CIRB domain of Trp3, −6, and −7 more effectively than to that of Trp1, −2, −4, and −5, suggesting that the closely related Trp3, −6, and −7 have higher affinity for the F2v domain and thus may be more sensitive to the activation by IP_3Rs than the rest of the Trp homologues. However, it is important to note that under resting Ca^{2+} concentrations of ~0.1 μM, all CIRB domains would prefer binding to F2v in the *in vitro* binding assay. Because it is not clear how CaM is tethered to the channel under resting conditions when the cytosolic Ca^{2+} concentration is low, it is difficult to predict whether the F2v domain alone is sufficient to displace CaM from all Trp channels in excised patches. The fact that a higher concentration of peptide F2v is needed to activate Trp4 than to activate Trp3 agrees well with the binding data, suggesting that when acting alone, F2v is a weak competitor for the CaM-Trp4 interaction. This supports our conclusion that peptide F2v activates Trp3 by displacing CaM from the common binding site.

CaM regulation through competition with another protein appears to be a common mechanism shared with other Ca^{2+}-permeable channels. Similar to Trp-based channels, a C-terminal site of the *N*-methyl-D-aspartate receptor binds to Ca^{2+}/CaM and actin-associated α-actinin. CaM inhibits whereas α-actinin promotes channel opening (50,51). A common binding site for Ca^{2+}/CaM and the C terminus of the olfactory cyclic nucleotide-gated channel has been found at the N terminus of the same channel. CaM binding disrupts the interdomain coupling between the N and C terminus and inactivates the channel (52). For these channels, it is not known whether CaM is tethered to the channels at rest and whether it plays any functional role without the presence of any physiological stimulus. To date, only Trp channels have been shown to be activated by removing or inhibiting CaM. The relatively harsh treatment may be effective in releasing the channel from inhibition by CaM, but this does not result in a complete activation of Trp channels (34). A full stimulation of Trp channels should therefore include multiple events, such as the activation of IP_3Rs, Ca^{2+} store-depletion, and perhaps the increase in the level of diacylglycerol.

Native SOCs may be regulated by IP_3Rs and CaM in a similar manner. However, because the single channel conductance of the endogenous channel is very low (12) and the channel density is much lower than the expressed Trp channels, it has been difficult for us to determine confidently whether or not similar mechanisms that stimulate the Trp channels also stimulate the native SOCs in control HEK cells. In A431 epithelial cells, IP_3 has been shown to activate SOCs via IP_3Rs (53). In whole-cell studies, intracellular infusion of CaM inhibited the SOC in bovine endothelial cells by slowing down the activation and speeding up the inactivation (54). Ca^{2+}-dependent inactivation has been documented for SOCs found in a number of different cells (55,56). Thus, conformational coupling involving IP_3Rs and its negative control via CaM may be a primary mechanism of gating for SOCs.

Acknowledgements

We thank Dr. Z. Chen for the initial characterization of Trp4 binding to IP_3R3 and CaM, D. Chuang for technical assistance, and Dr. K. Mikoshiba for cDNA of IP_3R1 and IP_3R3.

References

1. Putney JW Jr. Cell Calcium 1986;7:1–12. [PubMed: 2420465]
2. Putney JW Jr. Cell Calcium 1990;11:611–624. [PubMed: 1965707]
3. Berridge MJ. Biochem J 1995;312:1–11. [PubMed: 7492298]
4. Clapham DE. Cell 1995;80:259–268. [PubMed: 7834745]
5. Birnbaumer L, Zhu X, Jiang M, Boulay G, Peyton M, Vannier B, Brown D, Platano D, Sadeghi H, Stefani E, Birnbaumer M. Proc Natl Acad Sci U S A 1996;93:15195–15202. [PubMed: 8986787]
6. Zhu X, Jiang M, Peyton M, Boulay G, Hurst R, Stefani E, Birnbaumer L. Cell 1996;85:661–671. [PubMed: 8646775]
7. Hofmann T, Schaefer M, Schultz G, Gudermann T. J Mol Med 2000;78:14–25. [PubMed: 10759026]
8. Okada T, Inoue R, Yamazaki K, Maeda A, Kurosaki T, Yamakuni T, Tanaka I, Shimizu S, Ikenaka K, Imoto K, Mori Y. J Biol Chem 1999;274:27359–27370. [PubMed: 10488066]
9. Fasolato C, Innocenti B, Pozzan T. Trends Pharmacol Sci 1994;15:77–83. [PubMed: 8184490]
10. Zitt C, Obukhov AG, Strubing C, Zobel A, Kalkbrenner F, Luckhoff A, Schultz G. J Cell Biol 1997;138:1333–1341. [PubMed: 9298988]
11. Hofmann T, Obukhov AG, Schaefer M, Harteneck C, Gudermann T, Schultz G. Nature 1999;397:259–263. [PubMed: 9930701]
12. Kiselyov K, Xu X, Kuo TH, Mozhayeva G, Pessah I, Mignery G, Zhu X, Birnbaumer L, Muallem S. Nature 1998;396:478–482. [PubMed: 9853757]
13. Kiselyov K, Mignery GA, Zhu MX, Muallem S. Mol Cell 1999;4:423–429. [PubMed: 10518223]

14. Boulay G, Brown D, Qin N, Jiang M, Dietrich A, Zhu MX, Chen Z, Birnbaumer M, Mikoshiba K, Birnbaumer L. Proc Natl Acad Sci U S A 1999;96:14955–14960. [PubMed: 10611319]
15. Liu X, Wang W, Singh BB, Lockwich T, Jadlowiec J, O'Connell B, Wellner R, Zhu MX, Ambudkar IS. J Biol Chem 2000;275:3403–3411. [PubMed: 10652333]
16. Vannier B, Peyton M, Boulay G, Brown D, Qin N, Jiang M, Zhu X, Birnbaumer L. Proc Natl Acad Sci U S A 1999;96:2060–2064. [PubMed: 10051594]
17. Philipp S, Cavalie A, Freichel M, Wissenbach U, Zimmer S, Trost C, Marquart A, Murakami M, Flockerzi V. EMBO J 1996;15:6166–6171. [PubMed: 8947038]
18. Boulay G, Zhu X, Peyton M, Jiang M, Hurst R, Stefani E, Birnbaumer L. J Biol Chem 1997;272:29672–29680. [PubMed: 9368034]
19. Zhu X, Jiang M, Birnbaumer L. J Biol Chem 1998;273:133–142. [PubMed: 9417057]
20. Xu XZ, Chien F, Butler A, Salkoff L, Montell C. Neuron 2000;26:647–657. [PubMed: 10896160]
21. Li HS, Xu XZ, Montell C. Neuron 1999;24:261–273. [PubMed: 10677043]
22. Philipp S, Trost C, Warnat J, Rautmann J, Himmerkus N, Schroth G, Kretz O, Nastainczyk W, Cavalie A, Hoth M, Flockerzi V. J Biol Chem 2000;275:23965–23972. [PubMed: 10816590]
23. Lockwich TP, Liu X, Singh BB, Jadlowiec J, Weiland S, Ambudkar IS. J Biol Chem 2000;275:11934–11942. [PubMed: 10766822]
24. Rosado JA, Sage SO. Biochem J 2000;350:631–635. [PubMed: 10970773]
25. Chevesich J, Kreuz AJ, Montell C. Neuron 1997;18:95–105. [PubMed: 9010208]
26. Warr CG, Kelly LE. Biochem J 1996;314:497–503. [PubMed: 8670063]
27. Trost C, Marquart A, Zimmer S, Philipp S, Cavalie A, Flockerzi V. FEBS Lett 1999;451:257–263. [PubMed: 10371201]
28. Scott K, Sun Y, Beckingham K, Zuker CS. Cell 1997;91:375–383. [PubMed: 9363946]
29. Sanford J, Codina J, Birnbaumer L. J Biol Chem 1991;266:9570–9579. [PubMed: 1903391]
30. Qin N, Olcese R, Bransby M, Lin T, Birnbaumer L. Proc Natl Acad Sci U S A 1999;96:2435–2438. [PubMed: 10051660]
31. Lee SH, Kim JC, Lee MS, Heo WD, Seo HY, Yoon HW, Hong JC, Lee SY, Bahk JD, Hwang I, Cho MJ. J Biol Chem 1995;270:21806–21812. [PubMed: 7665602]
32. Erickson-Viitanen S, DeGrado WF. Methods Enzymol 1987;139:455–478. [PubMed: 3587035]
33. Tang Y, Tang J, Chen Z, Trost C, Flockerzi V, Li M, Ramesh V, Zhu MX. J Biol Chem 2000;275:37559–37564. [PubMed: 10980202]
34. Zhang Z, Tang J, Tikunova S, Johnson JD, Chen Z, Qin N, Dietrich A, Stefani E, Birnbaumer L, Zhu MX. Proc Natl Acad Sci U S A 2001;98:3168–3173. [PubMed: 11248050]
35. Randriamampita C, Tsien RY. Nature 1993;364:809–814. [PubMed: 8355806]
36. Csutora P, Su Z, Kim HY, Bugrim A, Cunningham KW, Nuccitelli R, Keizer JE, Hanley MR, Blalock JE, Marchase RB. Proc Natl Acad Sci U S A 1999;96:121–126. [PubMed: 9874782]
37. Trepakova ES, Csutora P, Hunton DL, Marchase RB, Cohen RA, Bolotina VM. J Biol Chem 2000;275:26158–26163. [PubMed: 10851243]
38. Yao Y, Ferrer-Montiel AV, Montal M, Tsien RY. Cell 1999;98:475–485. [PubMed: 10481912]
39. Patterson RL, van Rossum DB, Gill DL. Cell 1999;98:487–499. [PubMed: 10481913]
40. Meissner G, Lu X. Biosci Rep 1995;15:399–408. [PubMed: 8825041]
41. Irvine RF. FEBS Lett 1990;263:5–9. [PubMed: 2185036]
42. Vaca L, Kunze DL. Am J Physiol 1995;269:C733–C738. [PubMed: 7573404]
43. Kiselyov KI, Mamin AG, Semyonova SB, Mozhayeva GN. FEBS Lett 1997;407:309–312. [PubMed: 9175874]
44. Kiselyov KI, Semyonova SB, Mamin AG, Mozhayeva GN. Pflugers Arch 1999;437:305–314. [PubMed: 9929574]
45. Thrower EC, Mobasheri H, Dargan S, Marius P, Lea EJ, Dawson AP. J Biol Chem 2000;275:36049–36055. [PubMed: 10956640]
46. Ma HT, Patterson RL, van Rossum DB, Birnbaumer L, Mikoshiba K, Gill DL. Science 2000;287:1647–1651. [PubMed: 10698739]

47. Acharya JK, Jalink K, Hardy RW, Hartenstein V, Zuker CS. Neuron 1997;18:881–887. [PubMed: 9208856]
48. Raghu P, Colley NJ, Webel R, James T, Hasan G, Danin M, Selinger Z, Hardie RC. Mol Cell Neurosci 2000;15:429–445. [PubMed: 10833300]
49. Mery L, Magnino F, Schmidt K-H, Krause K, Dufour J-F. FEBS Lett 2001;487:377–383. [PubMed: 11163362]
50. Zhang S, Ehlers MD, Bernhardt JP, Su CT, Huganir RL. Neuron 1998;21:443–453. [PubMed: 9728925]
51. Krupp JJ, Vissel B, Thomas CG, Heinemann SF, Westbrook GL. J Neurosci 1999;19:1165–1178. [PubMed: 9952395]
52. Varnum MD, Zagotta WN. Science 1997;278:110–113. [PubMed: 9311913]
53. Zubov AI, Kaznacheeva EV, Nikolaev AV, Alexeenko VA, Kiselyov K, Muallem S, Mozhayeva GN. J Biol Chem 1999;274:25983–25985. [PubMed: 10473541]
54. Vaca L. FEBS Lett 1996;390:289–293. [PubMed: 8706879]
55. Zweifach A, Lewis RS. J Gen Physiol 1995;105:209–226. [PubMed: 7760017]
56. Liu X, O'Connell A, Ambudkar IS. J Biol Chem 1998;273:33295–33304. [PubMed: 9837902]

The abbreviations used are

IP_3
: inositol 1,4,5-trisphosphate

CaM
: calmodulin

CIRB
: CaM/IP_3 receptor binding

CMZ
: calmidazolium

EBFP
: enhanced blue fluorescence protein

GST
: glutathione *S*-transferase

hTrp1
: −3, −4, and −5, human Trp1, −3, −4, and −5, respectively

IP_3R
: IP_3 receptor

IP_3R3
: type 3 IP_3R

MBP
: maltose-binding protein

mTrp2
: −4, −5, −6, and −7, murine Trp2, −4, −5, −6, and −7, respectively

PCR
: polymerase chain reaction

SOC
: store-operated channel

MOPS

4-morpholinepropanesulfonic acid

HEDTA

N′-(2-hydroxyethyl)ethyl-enediamine-*N*,*N*,*N*′-triacetic acid

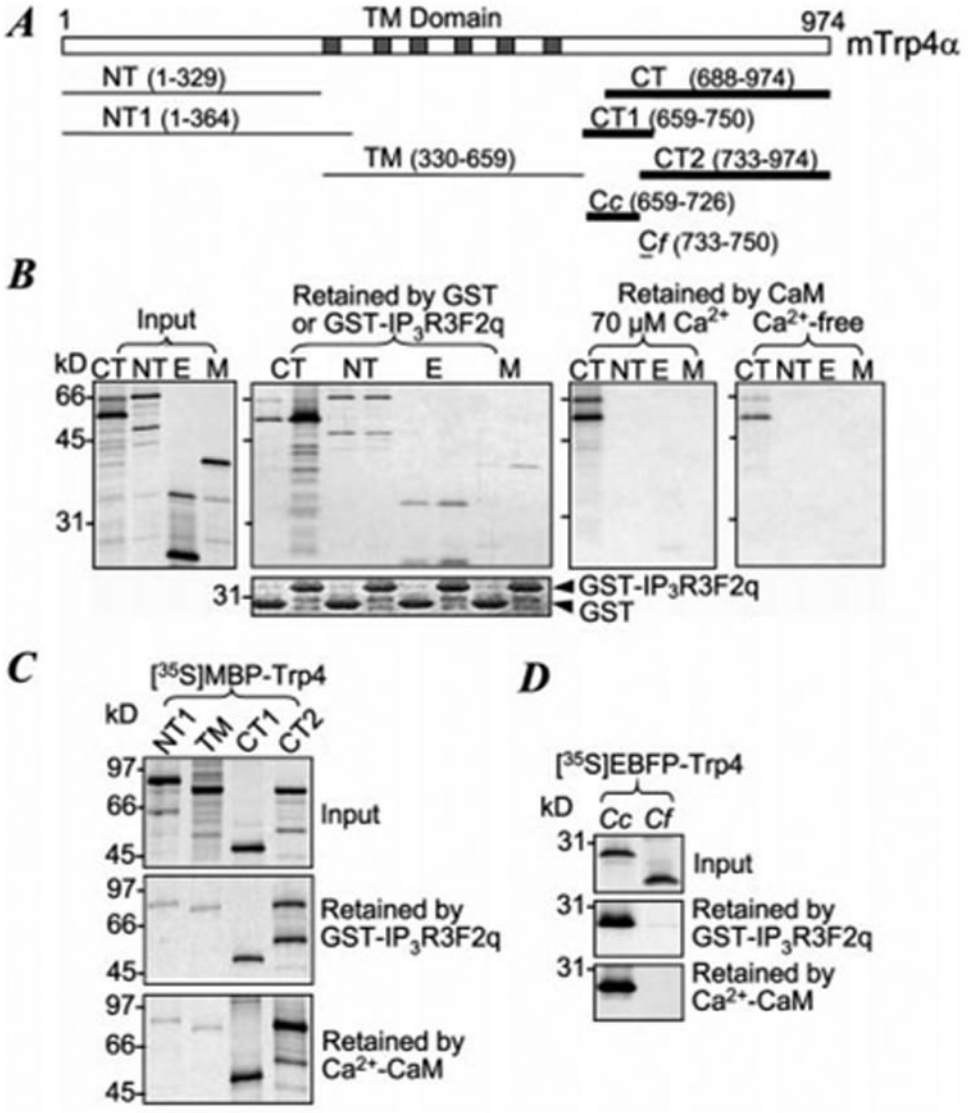

Fig. 1. Localization of IP_3R-binding domain and CaM-binding sites at the C terminus of mTrp4

A, diagram of mTrp4*α* and its fragments included in the EBFP or MBP fusion proteins. *Numbers* in *parentheses* indicate the positions of the fragments. *Thick* and *thin* lines denote that the binding to CaM is positive and negative, respectively. *Shaded boxes* in the full-length mTrp4*α* indicate the locations of trans-membrane (*TM*) segments. *B*, representative binding results showing the autoradiograms of input ^{35}S-labeled EBFP-Trp4 C-terminal (*CT*), MBP-Trp4 N-terminal (*NT*) fusion proteins, EBFP (*E*), and MBP (*M*) and those retained by GST, GST-IP_3R3F2q, and CaM. A picture of a Coomassie Blue-stained gel displayed *below* the *second panel* shows the amount of GST and GST fusion protein used. *C* and *D*, additional binding results showing that two C-terminal regions of mTrp4*α* (CT1 and CT2) (*C*) and Trp4C*c* (*D*) bind to both IP_3R3F2q and Ca^{2+}/CaM.

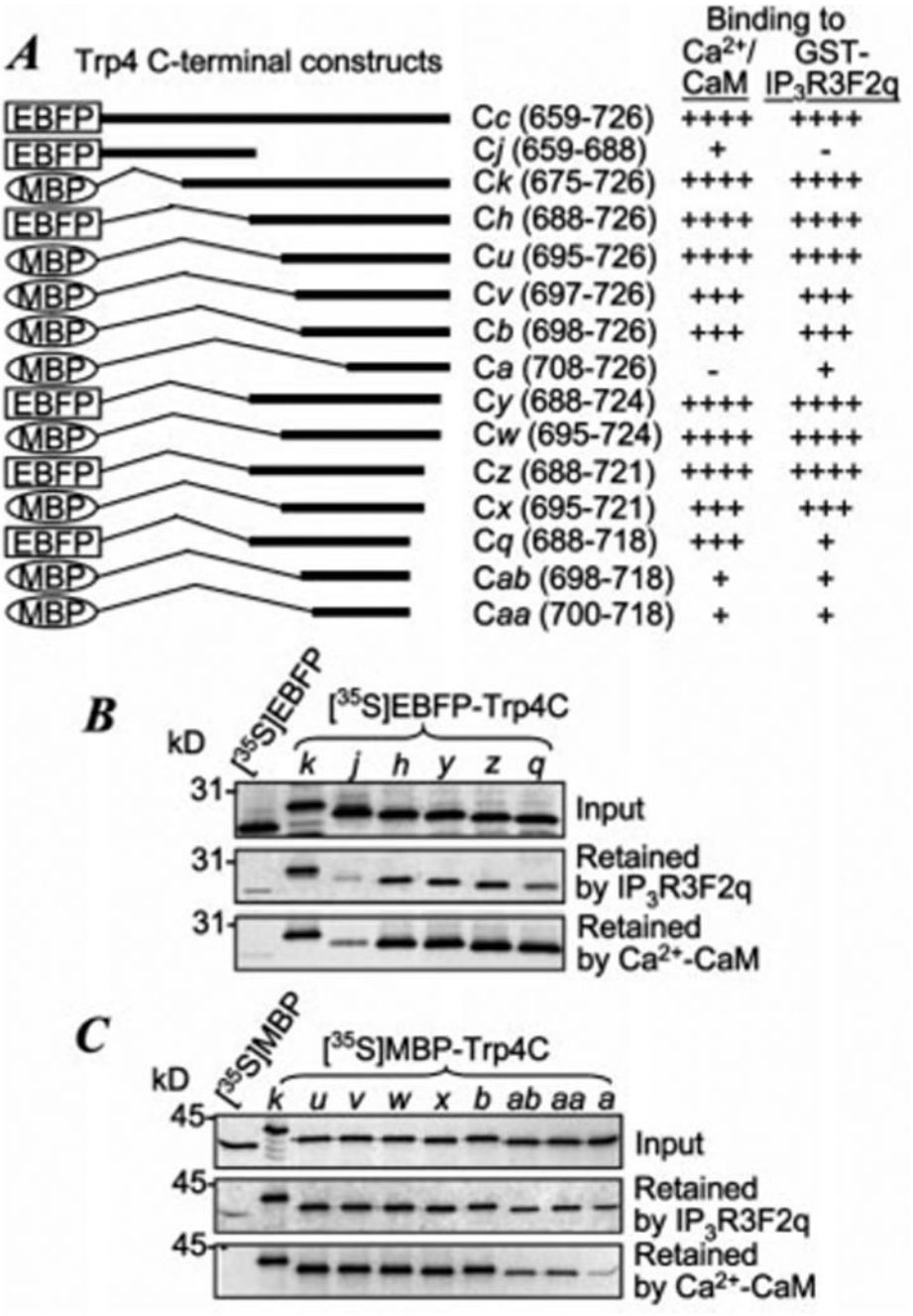

Fig. 2. Colocalization of binding sites for Ca^{2+}/CaM and IP_3R3F2q on Trp4CT1

A, compositions of EBFP or MBP fusion proteins containing subfragments of Trp4C*c*. Positions in the full-length mTrp4*α* are shown in *parentheses*. Relative intensities of the fusion proteins retained by Ca^{2+}/CaM and GST-IP_3R3F2q are indicated by the *plus* and *minus signs* and are summarized from 2–4 binding experiments. *B* and *C* show binding results from representative experiments.

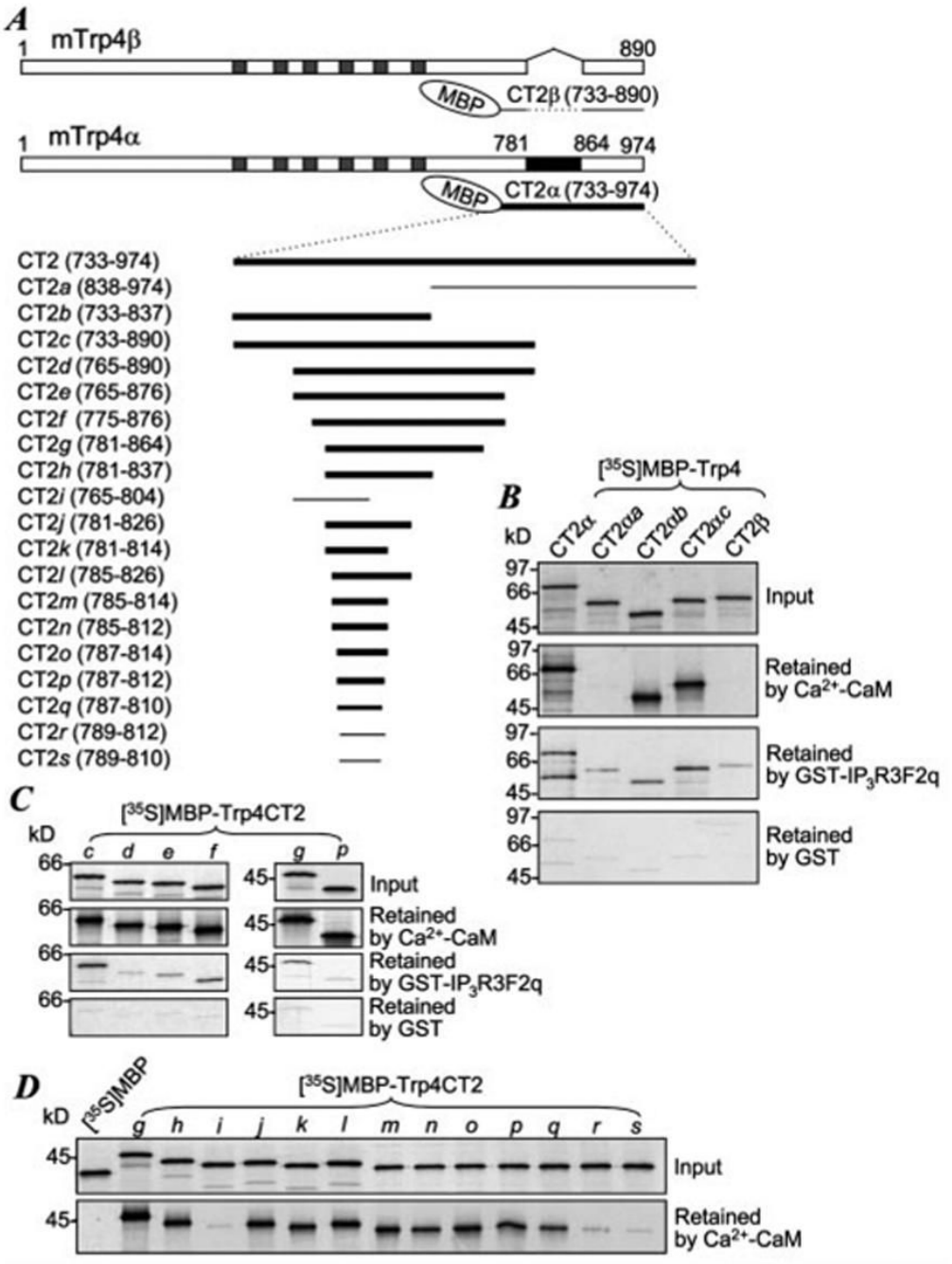

Fig. 3. Determination of binding sites for Ca^{2+}/CaM and IP_3R3F2q on Trp4CT2*α*

A, diagrams of mTrp4*α* and mTrp4*β* and compositions of MBP fusion proteins containing subfragments of Trp4CT2. Positions in respect to the full-length mTrp4*α* are shown in *parentheses*. CT2*β* contains the CT2 fragment of mTrp4*β* and lacks the 84-amino acid region (shown as a *dashed line* in MBP-CT2*β* and *black box* in mTrp4*α*). *Thick* and *thin lines* denote that the binding to CaM is positive and negative, respectively. *B–D* show binding results from representative experiments. Like Trp4CT2p, Trp4CT2h–o did not bind to GST-IP_3R3F2q (not shown).

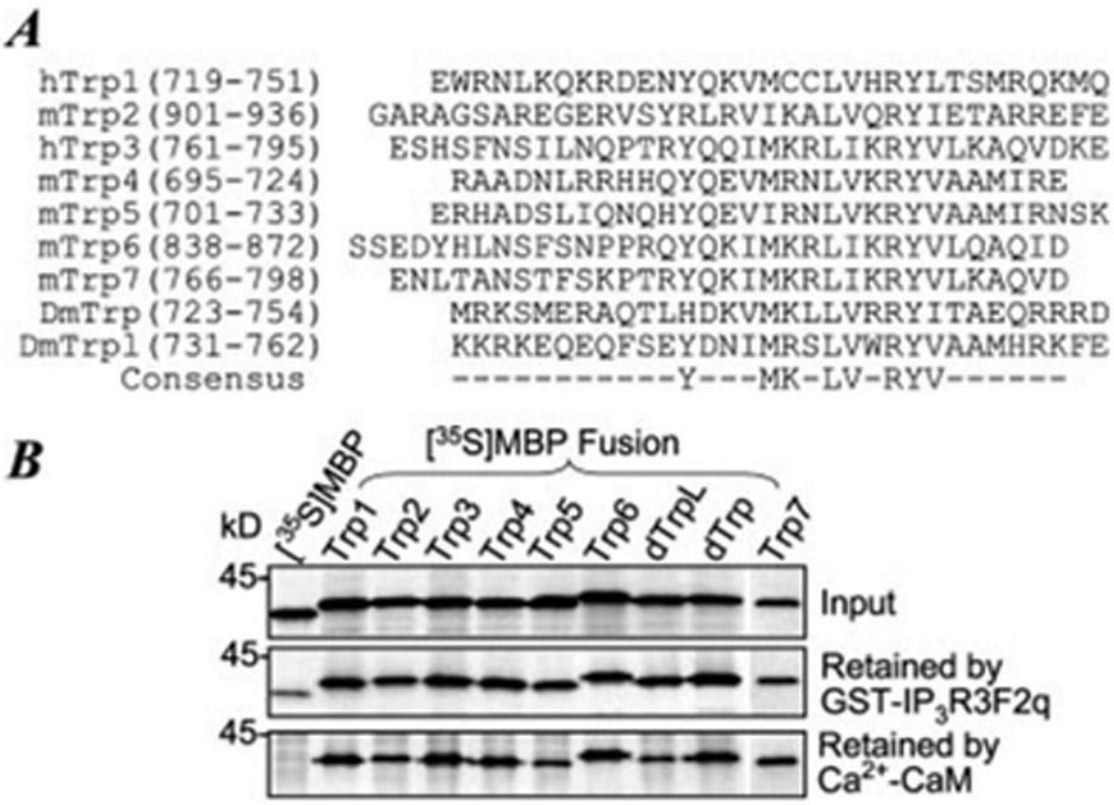

Fig. 4. The common CaM/IP$_3$R binding site is present in all Trp proteins

A, amino acid compositions of mammalian Trp1–7, *Drosophila* Trp (*DmTrp*), and TrpL (*DmTrpL*) present in the MBP fusion proteins. Positions for these sequences in the full-length proteins are shown in *parentheses*. ^{35}S-Labeled MBP fusion proteins were tested for binding to GST-IP$_3$R3F2q and to Ca^{2+}/CaM as described under "Materials and Methods." Representative binding results are shown in *B*.

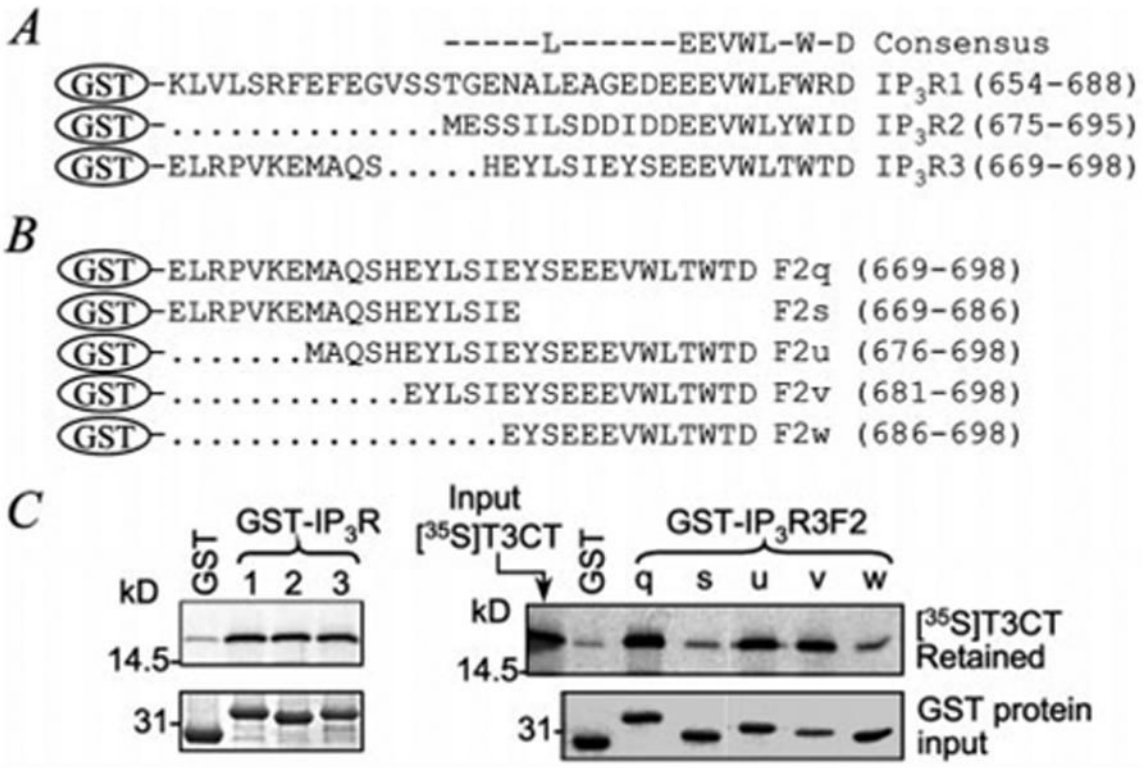

Fig. 5. All IP_3Rs interact with the C terminus of Trp3

A, amino acid compositions of IP_3R1, IP_3R2, and IP_3R3 included in the GST fusion proteins. *B*, amino acid compositions of subregions of IP_3R3F2q included in the GST fusion proteins. Positions in the full-length proteins are indicated in parentheses. ^{35}S-Labeled hTrp3 C terminus (T3CT, Asn^{725}–Glu^{848}) was tested for binding to the GST-IP_3R fusion proteins as described under "Materials and Methods." Representative binding results are shown in *C*. *Upper panels* show [^{35}S]T3CT retained by the GST fusion proteins as revealed by autoradiography, while *lower panels* show the amount of GST fusion proteins used as revealed by staining with Coomassie Blue.

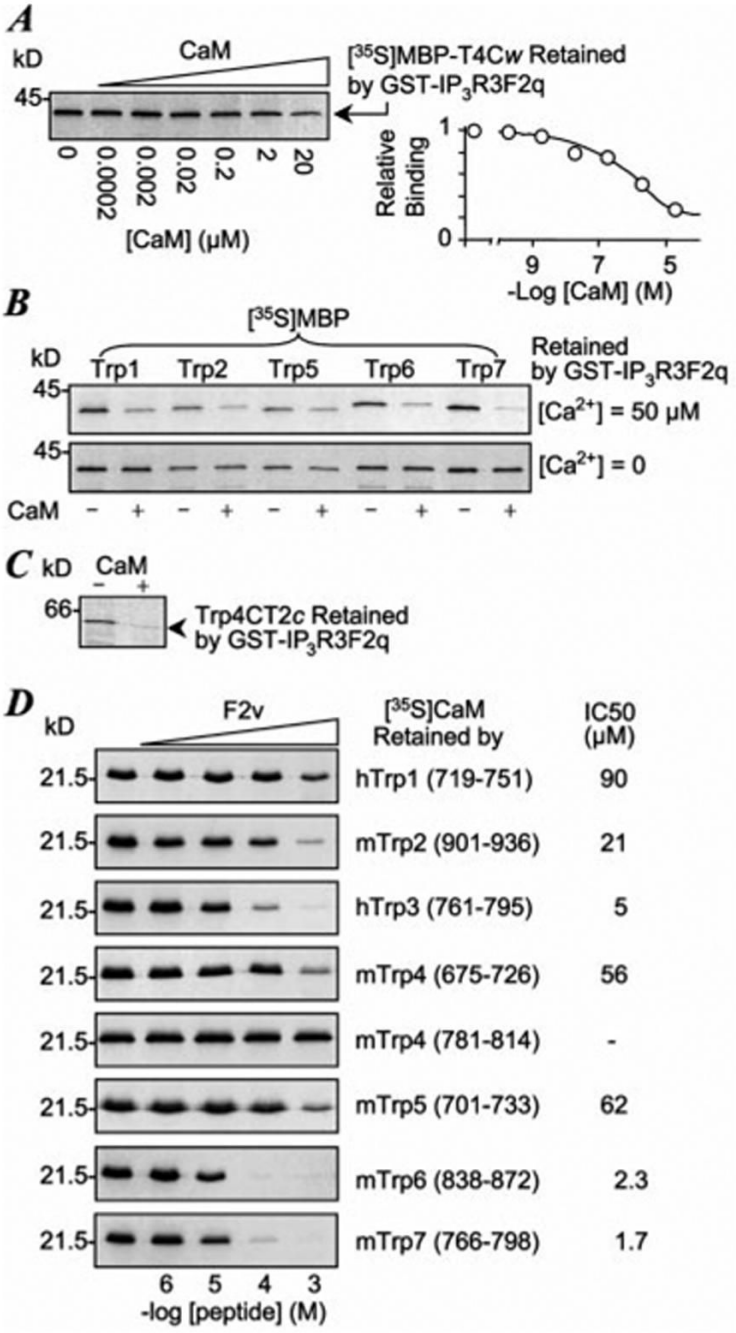

Fig. 6. Competition between CaM and IP_3R3 for binding to the Trp CIRB domains

A, CaM inhibits Trp4 binding to IP_3R3. Varying concentrations of CaM were included in the binding reactions for ^{35}S-labeled MBP-T4C*w* and GST-IP_3R3F2q. The binding buffer contained 70 μM free Ca^{2+}. After washing, bound [^{35}S]MBP-T4C*w* was separated by SDS-polyacrylamide gel electrophoresis. The *left panel* shows an autoradiogram from a representative experiment, while the *right panel* shows averages of results of phosphorimaging analysis of the relative amount of [^{35}S]T4C*w* retained from three experiments. The *curve* is the least-square fit of the equation, $y = 1/(1 + [P]/IC_{50})$, where y is relative binding, [P] is CaM concentration, and IC_{50} = 2.1 μM is the concentration that causes 50% inhibition. *B*, representative experiments show that 20 μM CaM inhibits the binding of IP_3R3F2q to the CIRB

domain of Trp1, −2, −5, −6, and −7 in a Ca^{2+}-dependent manner. 10 mM HEDTA and EGTA were used to buffer [Ca^{2+}] to 50 μM and 0 (<10 nM), respectively. *C*, binding of Trp4CT2c to IP_3R3F2q was inhibited by 20 μM CaM. [Ca^{2+}] = 50 μM. *D*, peptide F2v inhibits binding of CaM to the CIRB domain of Trp1–7. Varying concentrations of peptide F2v were included in the binding reaction for ^{35}S-labeled CaM and GST fusion proteins containing the CIRB sequence of Trp1–7 or the second CaM-binding site of Trp4 (CT2k, 781–814). Positions of Trp sequences included in the GST fusion proteins are indicated in *parentheses*. The binding buffer contained 70 μM free Ca^{2+}. After washing, bound [^{35}S]CaM was separated by SDS-polyacrylamide gel electrophoresis and revealed by autoradiography. IC_{50} values were determined from results of phosphorimaging analysis of the relative amount of [^{35}S]CaM retained by each Trp fragment from two or three experiments. The percentages of inhibitions for different concentrations of F2v were fitted with the equation as in *A*, except that [P] is the concentration of the peptide.

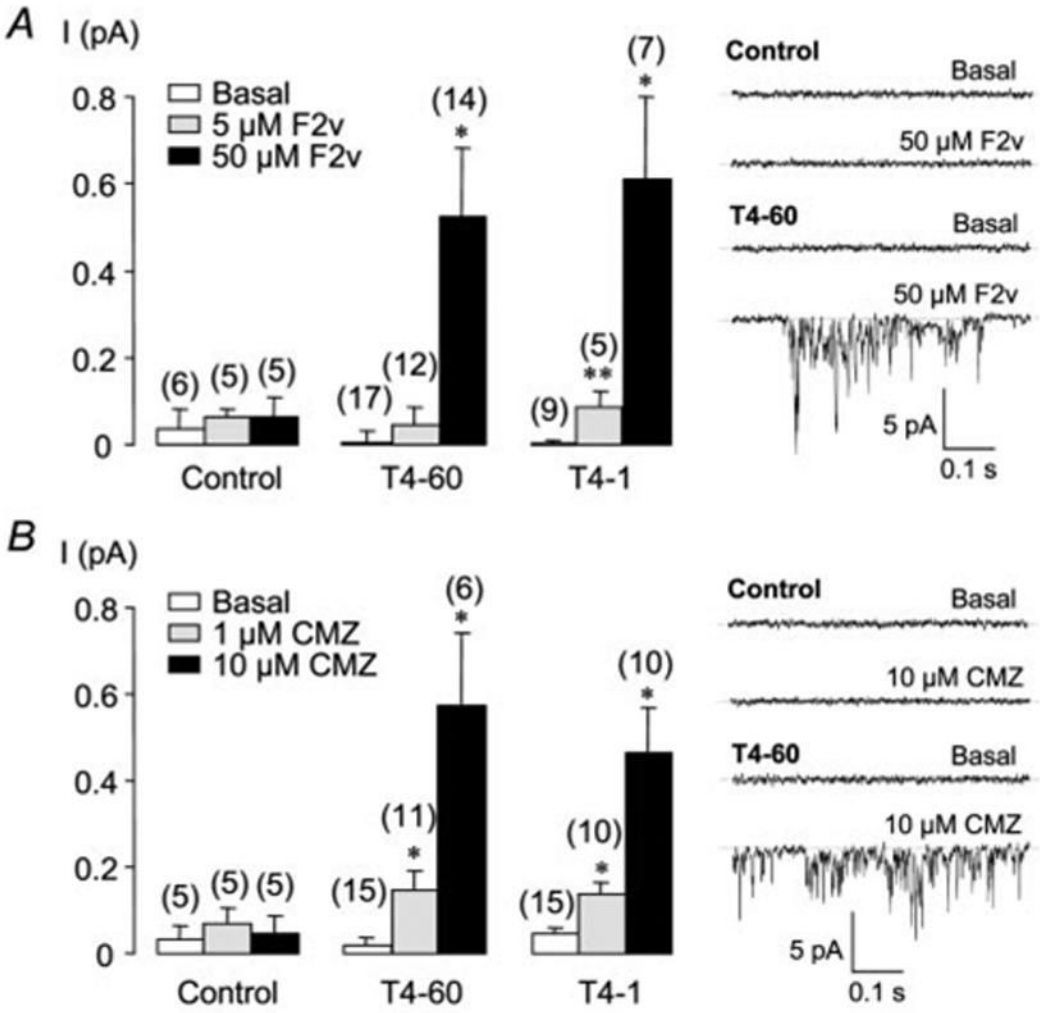

Fig. 7. Peptide F2v and CMZ stimulate channel activity in inside-out patches excised from Trp4

Inside-out patches were excised from untransfected HEK293 cells (control) or two stable cell lines expressing mTrp4*α* (T4–60 and T4–1) to a bath solution that contained either no Ca^{2+} (*A*) or 18 μM Ca^{2+} (*B*) as described under "Materials and Methods." Peptide F2v at 5 or 50 μM (*A*) and CMZ at 1 or 10 μM (*B*) were applied to the cytoplasmic side of the membrane by perfusion. *Bar graphs* show averages ± S.E. of the mean current (sampled from periods of 400 s) at −40 mV from the numbers of patches indicated in *parentheses*. Representative traces for control and T4–60 cells at basal level and 50 μM F2v (*A*) or 10 μM CMZ (*B*) are shown on the *right. Dashed lines* indicate closed level. *, $p < 0.01$; **, $p < 0.05$ different from basal level by Student's *t* test.

Table I

Affinities of Trp binding to CaM

Trp type	Amino acid sequences of synthetic peptides	Positions	K_d[a]	Ca^{2+} dependence[b]	
				K_{app}	n
			nM	*μM*	
hTrp1	WRNLKQKRDENYQKVMCCLVHRYLTSMRQK	720–749	30	12.9	2.6
mTrp2	GSAGEGERVSYRLRVIKALVQRYIETARRE	905–934	10	9.6	3.5
hTrp3	SFNSILNQPTRYQQIMKRLIKRYVLKAQVD	764–793	100	6.4	1.6
mTrp4	RAADNLRRHHQYQEVMRNLVKRYVAAMIRE	695–724	200	9.1	2.5
mTRP4	RKNLSLFDLTTLIHPRSAAIASERHN	787–812	600	1.0	1.7
mTrp5	RHADSLIQNQHYQEVIRNLVKRYVAAMIRN	702–731	220	44.2	1.5
mTrp6	HLNSFSNPPRQYQKIMKRLIKRYVLQAQID	843–872	290	5.0	1.9
mTrp7	TANSTFSKPTRYQKIMKRLIKRYVLKAQVD	769–798	19	1.6	2.5

[a] K_d for CaM was determined by the phosphodiesterase assay as described under “Materials and Methods” using the peptides shown.

[b] Ca^{2+} dependence was determined by *in vitro* binding assays using ^{35}S-labeled MBP fusion proteins shown in Fig. 4*A* and CaM-Sepharose. Free Ca^{2+} concentrations in the binding solutions were buffered by HEDTA or nitrilotriacetic acid (for mTrp5).